Available online at www.sciencedirect.com
ScienceDirect
Inorganica Chimica Acta 360 (2007) 2897–2904
Inorganica Chimica Acta
www.elsevier.com/locate/ica

Preparation and structural organisation of heteroleptic tetraphenylantimony(V) complexes comprising unidentately and bidentately coordinated *O*,*O*′-dialkyldithiophosphate groups: Multinuclear (^{13}C, ^{31}P) CP/MAS NMR and single-crystal X-ray diffraction studies

Maxim A. Ivanov [a], Oleg N. Antzutkin [b], Vladimir V. Sharutin [c], Alexander V. Ivanov [a,*], Antonya P. Pakusina [c], Mikhail A. Pushilin [d], Willis Forsling [b]

[a] *Institute of Geology and Nature Management, Far Eastern Branch of the Russian Academy of Sciences, 675000 Blagoveschensk, Amur Region, Russia*
[b] *Division of Chemistry, Luleå University of Technology, S-97187 Luleå, Sweden*
[c] *Blagoveschensk State Pedagogical University, 675000 Blagoveschensk, Amur Region, Russia*
[d] *Institute of Chemistry, Far Eastern Branch of the Russian Academy of Sciences, 690022 Vladivostok, Russia*

Received 2 August 2006; accepted 7 February 2007
Available online 12 March 2007

Abstract

O,*O*′-dipropyldithiophosphate and *O*,*O*′-di-*iso*-butyldithiophosphate (Dtph) tetraphenylantimony(V) complexes of the general formula $[Sb(C_6H_5)_4\{S_2P(OR)_2\}]$ ($R = C_3H_7$, i-C_4H_9) were prepared and studied by means of ^{13}C, ^{31}P CP/MAS NMR spectroscopy and single-crystal X-ray diffraction. Distorted octahedral and trigonal bipyramidal molecular structures have been established for prepared complexes. These unexpected structural distinctions between chemically related compounds are defined by the principally different coordination modes of *O*,*O*′-dipropyldithiophosphate and *O*,*O*′-di-*iso*-butyldithiophosphate ligands in their molecular structures (i.e., *S*,*S*′-bidentate chelating and *S*-unidentately coordinated, respectively). To characterise quantitatively phosphorus sites in both species of dithiophosphate ligands, ^{31}P chemical shift anisotropy parameters (δ_{aniso} and η) were calculated from spinning sideband manifolds in MAS NMR spectra. The ^{31}P chemical shift tensors for the bidentate chelating and unidentately coordinated dithiophosphate ligands display a profoundly rhombic and nearly axially symmetric characters, respectively.

Keywords: Heteroleptic dialkyldithiophosphate tetraphenylantimony(V) complexes; Molecular structures; ^{13}C, ^{31}P CP/MAS NMR spectroscopy; ^{31}P chemical shift anisotropy; Single-crystal X-ray diffraction

1. Introduction

Organoantimony compounds are of interest as biocides, fungicides, catalyst components and antioxidants [1]. Therefore, syntheses of new organoantimony compounds and studies of their structures and properties are of interest in modern coordination chemistry. Recently, we reported the preparation, heteronuclear (^{13}C, ^{15}N) CP/MAS NMR and structural studies of polycrystalline heteroleptic *N*,*N*-dialkyldithiocarbamate tetra-*p*-tolylantimony(V) and tetraphenylantimony(V) complexes of the general formulas $[Sb(p\text{-}CH_3\text{–}C_6H_4)_4(S_2CNR_2)]$ and $[Sb(C_6H_5)_4(S_2CNR_2)]$, where $R = CH_3$, C_2H_5, C_3H_7 and $R_2 = (CH_2)_6$ [2–4]. Distorted octahedral molecular structures with *S*,*S*′-bidentate

* Corresponding author. Tel.: +07 4162 527232; fax: +07 4162 534618.
E-mail addresses: Oleg.Antzutkin@ltu.se (O.N. Antzutkin), vvsharutin@rambler.ru (V.V. Sharutin), alexander.v.ivanov@chemist.com (A.V. Ivanov), pumalych@ich.dvo.ru (M.A. Pushilin), Willis.Forsling@ltu.se (W. Forsling).

0020-1693/$ - see front matter © 2007 Elsevier B.V. All rights reserved.
doi:10.1016/j.ica.2007.02.044

coordination mode of *N*,*N*-dialkyldithiocarbamate ligands were established for all named heteroleptic complexes. Moreover, in the unit cell of $[Sb(C_6H_5)_4\{S_2CN(CH_2)_6\}]$, two molecular forms of this complex, which are related to each other as conformational isomers, have been discovered using single-crystal X-ray diffraction analysis. Besides that, ^{13}C and ^{15}N resonance lines were assigned to the structural positions of corresponding atoms in the =N–C(S)S– groups of both conformers.

This article reports the preparation, multinuclear (^{31}P, ^{13}C) CP/MAS NMR and single-crystal X-ray diffraction studies on two novel heteroleptic tetraphenylantimony(V) complexes, $[Sb(C_6H_5)_4\{S_2P(OR)_2\}]$ (where $R = C_3H_7$ (**1**) and *i*-C_4H_9 (**2**)) comprising symmetrically disubstituted *O*,*O*′-dialkyldithiophosphate ligands. The principally different coordination modes of *O*,*O*′-dipropyldithiophosphate and *O*,*O*′-di-*iso*-butyldithiophosphate ligands (i.e., *S*,*S*′-bidentate chelating and S-unidentately coordinated, respectively) have been established for these two chemically related compounds, which are characterised by either a distorted octahedral (**1**) or a trigonally bipyramidal (**2**) molecular structures. Spinning sideband patterns, which were observed in ^{31}P MAS NMR spectra of both compounds **1** and **2**, display either mainly rhombic or profound axially symmetric characters of the ^{31}P chemical shift tensors for bidentate chelating and unidentately coordinated dithiophosphate ligands, respectively. To characterise quantitatively the phosphorus sites in both species of dithiophosphate ligands, ^{31}P chemical shift anisotropy parameters (δ_{aniso} and η) were successfully calculated from spinning sideband manifolds. Correlations between resolved molecular structures of both tetraphenylantimony(V) complexes and ^{31}P NMR data are also discussed.

2. Experimental

2.1. Materials

Two potassium salts of symmetrically disubstituted *O*,*O*′-dialkyldithiophosphoric acids, which constitute the major components of the commercial collectors Danafloats, were provided to us by 'CHEMINOVA AGRO A/S':

O,*O*′-di-*n*-propyldithiophosphate – $K\{S_2P(OC_3H_7)_2\}$ – Danafloat-133 K.
O,*O*′-di-*i*-butyldithiophosphate – $K\{S_2P(O\text{-}i\text{-}C_4H_9)_2\}$ – Danafloat-245 K.

2.2. Synthesis of polycrystalline complexes

O,*O*′-Dialkyldithiophosphate tetraphenylantimony(V) complexes, $[Sb(C_6H_5)_4\{S_2P(OR)_2\}]$ (**1**) ($R = C_3H_7$) and (**2**) ($R = i\text{-}C_4H_9$), were prepared by mixing aqueous solutions of $[Sb(C_6H_5)_4]Cl$ and an excess (~10%) of the corresponding potassium dialkyldithiophosphate, $K\{S_2P(OR)_2\}$. The resulting yellowish-white precipitates were collected by filtration, washed with water, dried naturally and recrystallised from benzene–heptane (1:1) solutions. Both heteroleptic tetraphenylantimony(V) compounds **1** and **2**, as well as the original potassium salts, were comparatively characterised on solid state ^{13}C CP/MAS NMR data (δ, ppm):

$[Sb(C_6H_5)_4\{S_2P(OC_3H_7)_2\}]$(**1**): 149.4, 136.6, 134.9, 132.9, 131.6, 130.5, 129.5, 128.6 (C_6H_5–); 66.7, 65.7 (1:1, –OCH_2–); 25.3, 24.8 (1:1, –CH_2–); 11.9, 10.0 (1:1, –CH_3). Cf. data for the original $K\{S_2P(OC_3H_7)_2\}$: 71.7, 68.9, 68.8 (2:1:1, –OCH_2–); 25.0, 24.1 (1:1, –CH_2–); 10.2, 9.9, 8.9 (1:2:1, –CH_3).

$[Sb(C_6H_5)_4\{S_2P(O\text{-}i\text{-}C_4H_9)_2\}]$ (**2**): *, 138.4, 135.3, 133.1, 130.8, 130.1, 129.7 (C_6H_5–); 73.1, 71.2 (1:1, –OCH_2–); 30.1, 29.5 (1:1, –CH=); 20.6, 20.1, 19.6, 17.9 (1:1:1:1, –CH_3). (*^{13}C resonance lines assigned to ≡C–Sb are too broad to determine the corresponding chemical shifts.) Cf. data for the original $K\{S_2P(O\text{-}i\text{-}C_4H_9)_2\}$: (1:1:2) – 75.1, 74.2, 73.5, 73.2, 72.9 (–OCH_2–); 29.9, 29.8, 29.7 (–CH=); 21.1, 21.0, 20.9, 20.8, 20.7, 20.6, 20.4, 20.3, 20.2, 20.1 (–CH_3).

For X-ray diffraction studies, suitable single crystals of (*O*,*O*′-dipropyldithiophosphato-*S*,*S*′)tetraphenylantimony (V), $[Sb(C_6H_5)_4\{S_2P(OC_3H_7)_2\}]$ (**1**) and (*O*,*O*′-di-*iso*-butyldithiophosphato-*S*)tetraphenylantimony(V), $[Sb(C_6H_5)_4\{S_2P(O\text{-}i\text{-}C_4H_9)_2\}]$ (**2**) were prepared using recrystallisation of precipitated complexes from benzene–heptane (1:1) solutions at room temperature. Both complexes **1** and **2** have been isolated as prismatic transparent and colourless crystals. Yield (**1**) 71%. *Anal.* Calc. for $C_{30}H_{34}O_2PS_2Sb$ ($M_r = 643.41$): C, 55.99; H, 5.29; Sb, 18.97. Found: C, 55.81; H, 4.18; Sb, 18.88%. Yield (**2**), 66%. *Anal.* Calc. for $C_{32}H_{38}O_2PS_2Sb$ ($M_r = 671.46$): C, 57.23; H, 5.66; Sb, 18.18. Found: C, 57.15; H, 5.71; Sb, 18.13%.

2.3. Physical measurements

2.3.1. ^{13}C and ^{31}P CP/MAS NMR spectroscopy

Solid state ^{13}C and ^{31}P magic-angle-spinning (MAS) NMR spectra were recorded on a Varian/Chemagnetics InfinityPlus CMX-360 ($B_0 = 8.46$ T) spectrometer operating in the pulsed Fourier transform mode, using cross-polarisation (CP) from the protons together with proton decoupling [5]. The $^{13}C/^{31}P$ operating frequencies were 90.52/145.73 MHz, respectively. The proton $\pi/2$ pulse durations were 5.2/5.2 μs, CP mixing times were 1.5/4.5 ms and the nutation frequencies of protons during decoupling $\omega_{nut}/2\pi = 43/47$ kHz. For each sample, 3600–7500/380–2000 transients, spaced by relaxation delays of 2.5/3.0 s, were accumulated. Polycrystalline samples (ca. 350 mg) were packed in zirconium dioxide standard double bearing 7.5 mm rotors. The spinning frequencies for studied samples ranged from 4200 to 4500/3000 to 4000 Hz and were stabilised to ±2 Hz using a built-in stabilisation device. All ^{13}C and ^{31}P NMR spectra were recorded at room temperature (ca. 295 K).

^{13}C Isotropic chemical shifts (in the deshielding, δ-scale) were externally referenced to the least shielded resonance of solid adamantane at 38.56 ppm relative to tetramethylsilane [6]. Chemical shifts and integrated

intensity ratios for overlapping signals in the ^{13}C NMR spectra were additionally refined by fragment-by-fragment simulations taking into account both line positions and line widths, as well as the Lorentzian and Gaussian contributions to the line shapes. All ^{31}P chemical shift data are given with respect to 85.5% H_3PO_4 [7] (here, 0 ppm, externally referenced), which was mounted in a short 1 mm glass tube and placed in a 7.5 mm rotor to avoid errors due to differences in the magnetic susceptibility. Drifts in the $^{13}C/^{31}P$ frequencies (B_0-drift) were 0.051/0.11 Hz h^{-1}, respectively. The homogeneity of the magnetic field was monitored by measuring the width of the reference signal of crystalline adamantane at $\delta(^{13}C) = 38.56$ ppm, which was 2.6 Hz.

The anisotropy, $\delta_{aniso} = \delta_{zz} - \delta_{iso}$, and the asymmetry parameter of ^{31}P chemical shift tensor (CST), $\eta = (\delta_{yy} - \delta_{xx})/(\delta_{zz} - \delta_{iso})$, were estimated from the determined ratios between integrated sideband intensities for each phosphorus site in the NMR spectra recorded at two different spinning frequencies using a simulation program in the Mathematica front end [8]. To increase the number of spinning sidebands (>10) in ^{31}P NMR spectra, which is needed for more accurate estimation of CSA parameters, spectra were also recorded at low spinning frequencies (1–3 kHz).

Table 1
Selected crystal data for $[Sb(C_6H_5)_4\{S_2P(OC_3H_7)_2\}]$ (**1**) and $[Sb(C_6H_5)_4\{S_2P(O\text{-}i\text{-}C_4H_9)_2\}]$ (**2**)

Empirical formula	$C_{30}H_{34}O_2PS_2Sb$	$C_{32}H_{38}O_2PS_2Sb$
Formula weight	643.41	671.46
Crystal system	monoclinic	triclinic
Space group	$P2_1/n$	$P\bar{1}$
Crystal shape	prism	prism
Crystal size (mm)	$0.26 \times 0.25 \times 0.18$	$0.32 \times 0.26 \times 0.18$
Unit cell dimensions		
a (Å)	11.0359(3)	9.2220(5)
b (Å)	12.4279(4)	9.4371(5)
c (Å)	21.6507(7)	19.004(1)
α (°)	90.000	83.817(1)
β (°)	95.604(1)	77.966(1)
γ (°)	90.000	87.759(1)
V (Å^3)	2955.3(2)	1607.9(2)
Z	4	2
D_{calc} (g cm^{-3})	1.446	1.387
Temperature (K)	173(1)	173(1)
μ (Mo Kα) (mm^{-1})	1.154	1.064
θ Range	2.47–31.53	2.71–31.52
Range of h, k and l	$-15 \rightarrow 16$, $-18 \rightarrow 18$, $-31 \rightarrow 29$	$-13 \rightarrow 13$, $-13 \rightarrow 13$, $-27 \rightarrow 27$
F(000)	1312	688
R_{int}	0.0374	0.0293
Number of observations	8150	9412
Criterion of significance	$I > 2\sigma(I)$	$I > 2\sigma(I)$
Number of parameters	327	347
Weighting scheme	$w = 1/[s^2(F_o^2) + (0.0307P)^2 + 1.7993P]$, where $P = (F_o^2 + 2F_c^2)/3$	$w = 1/[s^2(F_o^2) + (0.0446P)^2 + 0.9291P]$, where $P = (F_o^2 + 2F_c^2)/3$
S (goodness-of-fit)	1.087	1.069
R_1, wR_2 ($F^2 > 2\sigma(F^2)$)	0.0309, 0.0708	0.0339, 0.0835
$\Delta\rho_{max}$, $\Delta\rho_{min}$ (e/Å^3)	1.348, −0.544	1.799, −0.674

2.3.2. Crystal structure determination

Suitable single crystals of **1** and **2** $[Sb(C_6H_5)_4\{S_2P(OR)_2\}]$ ($R = C_3H_7$ and i-C_4H_9) were selected and

Table 2
Selected bond lengths (Å) and bond angles (°) for $[Sb(C_6H_5)_4\{S_2P(OC_3H_7)_2\}]$ (**1**)

Bond lengths			
Sb–C(11)	2.126(1)	C(14)–C(15)	1.377(2)
Sb–C(21)	2.123(1)	C(15)–C(16)	1.389(2)
Sb–C(31)	2.149(1)	C(21)–C(22)	1.394(2)
Sb–C(41)	2.128(1)	C(21)–C(26)	1.388(2)
Sb–S(1)	3.0060(4)	C(22)–C(23)	1.392(2)
Sb–S(2)	3.5571(4)	C(23)–C(24)	1.382(2)
S(1)–P	1.9981(5)	C(24)–C(25)	1.381(2)
S(2)–P	1.9577(5)	C(25)–C(26)	1.390(2)
P–O(1)	1.601(1)	C(31)–C(32)	1.396(2)
P–O(2)	1.602(1)	C(31)–C(36)	1.392(2)
O(1)–C(1)	1.451(2)	C(32)–C(33)	1.391(2)
O(2)–C(4)	1.456(2)	C(33)–C(34)	1.375(2)
C(1)–C(2)	1.496(2)	C(34)–C(35)	1.387(2)
C(2)–C(3)	1.521(2)	C(35)–C(36)	1.391(2)
C(4)–C(5)	1.507(2)	C(41)–C(42)	1.398(2)
C(5)–C(6)	1.491(3)	C(41)–C(46)	1.392(2)
C(11)–C(12)	1.384(2)	C(42)–C(43)	1.391(2)
C(11)–C(16)	1.390(2)	C(43)–C(44)	1.378(3)
C(12)–C(13)	1.397(2)	C(44)–C(45)	1.385(2)
C(13)–C(14)	1.374(3)	C(45)–C(46)	1.395(2)
Bond angles			
S(1)–Sb–S(2)	60.943(9)	C(11)–C(12)–C(13)	118.9(2)
P–S(1)–Sb	99.08(2)	C(12)–C(11)–C(16)	120.9(1)
P–S(2)–Sb	83.56(2)	C(13)–C(14)–C(15)	120.2(2)
S(1)–P–S(2)	116.39(2)	C(14)–C(13)–C(12)	120.5(2)
O(1)–P–S(1)	109.70(4)	C(14)–C(15)–C(16)	120.5(2)
O(1)–P–S(2)	111.82(4)	C(15)–C(16)–C(11)	119.0(1)
O(2)–P–S(1)	109.78(4)	C(22)–C(21)–Sb	121.8(1)
O(2)–P–S(2)	112.44(5)	C(26)–C(21)–Sb	117.7(1)
O(1)–P–O(2)	94.59(6)	C(21)–C(26)–C(25)	120.0(1)
C(1)–O(1)–P	118.97(9)	C(23)–C(22)–C(21)	119.2(1)
C(4)–O(2)–P	117.6(1)	C(24)–C(23)–C(22)	120.0(1)
O(1)–C(1)–C(2)	108.9(1)	C(24)–C(25)–C(26)	119.6(2)
C(1)–C(2)–C(3)	112.2(1)	C(25)–C(24)–C(23)	120.8(2)
O(2)–C(4)–C(5)	110.0(1)	C(26)–C(21)–C(22)	120.3(1)
C(4)–C(5)–C(6)	113.7(2)	C(32)–C(31)–Sb	120.6(1)
C(11)–Sb–S(1)	79.80(4)	C(36)–C(31)–Sb	120.5(1)
C(21)–Sb–S(1)	80.87(4)	C(33)–C(32)–C(31)	120.2(1)
C(31)–Sb–S(1)	172.27(4)	C(33)–C(34)–C(35)	119.8(1)
C(41)–Sb–S(1)	87.85(4)	C(34)–C(33)–C(32)	120.6(2)
C(11)–Sb–S(2)	71.04(4)	C(34)–C(35)–C(36)	120.1(2)
C(21)–Sb–S(2)	70.00(3)	C(35)–C(36)–C(31)	120.4(1)
C(31)–Sb–S(2)	111.41(4)	C(36)–C(31)–C(32)	118.9(1)
C(41)–Sb–S(2)	148.79(4)	C(42)–C(41)–Sb	118.0(1)
C(11)–Sb–C(21)	141.04(5)	C(46)–C(41)–Sb	122.6(1)
C(11)–Sb–C(31)	96.88(5)	C(41)–C(46)–C(45)	120.2(1)
C(11)–Sb–C(41)	106.10(5)	C(43)–C(42)–C(41)	119.8(2)
C(21)–Sb–C(31)	97.83(5)	C(43)–C(44)–C(45)	120.1(1)
C(21)–Sb–C(41)	106.62(5)	C(44)–C(43)–C(42)	120.6(2)
C(31)–Sb–C(41)	99.80(5)	C(44)–C(45)–C(46)	119.9(2)
C(12)–C(11)–Sb	117.6(1)	C(46)–C(41)–C(42)	119.4(1)
C(16)–C(11)–Sb	121.2(1)		

mounted on glass fibres with epoxy glue. Experimental intensity data were collected at $T = 173(1)$ K for both compounds **1** and **2** on a BRUKER SMART 1000 CCD diffractometer with graphite monochromated Mo Kα radiation ($\lambda = 0.71073$ Å) [9] (crystal-detector distance 45 mm). For compounds **1/2**, data were collected in series of 906/606 frames at $\varphi = 0°$, 90° and 180°/0°, 90°, 180° and 270°; ω scan with an increment of 0.2°/0.3° and an exposure time of 20 s/20 s per frame was used. Intensity data were corrected for absorption using the indices of equivalent reflections. The unit cell dimensions, additional crystallographic data and refinement results for the complexes are given in Table 1.

Table 3
Selected bond lengths (Å) and bond angles (°) for $[Sb(C_6H_5)_4\{S_2P(O\text{-}i\text{-}C_4H_9)_2\}]$ (**2**)

Bond lengths			
Sb–C(11)	2.147(1)	C(14)–C(15)	1.369(3)
Sb–C(21)	2.114(1)	C(15)–C(16)	1.400(2)
Sb–C(31)	2.104(1)	C(21)–C(22)	1.384(2)
Sb–C(41)	2.115(1)	C(21)–C(26)	1.391(2)
Sb–S(1)	2.9092(4)	C(22)–C(23)	1.393(3)
S(1)–P	2.0018(6)	C(23)–C(24)	1.377(3)
S(2)–P	1.9450(6)	C(24)–C(25)	1.383(3)
P–O(1)	1.606(1)	C(25)–C(26)	1.394(3)
P–O(2)	1.593(2)	C(31)–C(32)	1.383(2)
O(1)–C(1)	1.473(2)	C(31)–C(36)	1.392(2)
O(2)–C(5)	1.434(3)	C(32)–C(33)	1.395(2)
C(1)–C(2)	1.497(3)	C(33)–C(34)	1.386(3)
C(2)–C(3)	1.532(3)	C(34)–C(35)	1.372(3)
C(2)–C(4)	1.470(4)	C(35)–C(36)	1.389(2)
C(5)–C(6)	1.477(4)	C(41)–C(42)	1.386(2)
C(6)–C(7)	1.494(4)	C(41)–C(46)	1.393(2)
C(6)–C(8)	1.531(4)	C(42)–C(43)	1.390(2)
C(11)–C(12)	1.394(2)	C(43)–C(44)	1.371(3)
C(11)–C(16)	1.389(2)	C(44)–C(45)	1.381(3)
C(12)–C(13)	1.390(2)	C(45)–C(46)	1.395(2)
C(13)–C(14)	1.383(3)	Sb···O(1)	3.641(1)
Bond angles			
P–S(1)–Sb	109.92(2)	C(11)–C(16)–C(15)	119.8(2)
S(2)–P–S(1)	117.62(3)	C(16)–C(11)–C(12)	119.0(1)
O(1)–P–S(1)	105.84(5)	C(22)–C(21)–Sb	120.1(1)
O(1)–P–S(2)	112.82(5)	C(26)–C(21)–Sb	118.9(1)
O(2)–P–S(1)	108.50(6)	C(21)–C(22)–C(23)	119.0(2)
O(2)–P–S(2)	106.95(6)	C(24)–C(23)–C(22)	120.6(2)
O(1)–P–O(2)	104.26(9)	C(23)–C(24)–C(25)	120.2(2)
C(1)–O(1)–P	121.7(1)	C(24)–C(25)–C(26)	120.2(2)
O(1)–C(1)–C(2)	109.2(2)	C(21)–C(26)–C(25)	119.0(2)
C(1)–C(2)–C(3)	108.4(2)	C(22)–C(21)–C(26)	121.0(1)
C(1)–C(2)–C(4)	114.2(2)	C(32)–C(31)–Sb	118.2(1)
C(4)–C(2)–C(3)	111.7(2)	C(36)–C(31)–Sb	121.3(1)
C(5)–O(2)–P	121.7(1)	C(31)–C(32)–C(33)	119.2(2)
O(2)–C(5)–C(6)	110.5(2)	C(34)–C(33)–C(32)	120.2(2)
C(5)–C(6)–C(7)	110.5(3)	C(35)–C(34)–C(33)	120.2(2)
C(5)–C(6)–C(8)	109.5(2)	C(34)–C(35)–C(36)	120.3(2)
C(7)–C(6)–C(8)	111.1(2)	C(35)–C(36)–C(31)	119.6(2)
C(11)–Sb–S(1)	176.23(4)	C(32)–C(31)–C(36)	120.5(1)
C(21)–Sb–S(1)	82.42(4)	C(42)–C(41)–Sb	122.1(1)
C(31)–Sb–S(1)	78.45(4)	C(46)–C(41)–Sb	117.0(1)
C(41)–Sb–S(1)	86.79(4)	C(41)–C(42)–C(43)	119.0(2)
C(11)–Sb–C(21)	99.01(6)	C(44)–C(43)–C(42)	120.6(2)
C(11)–Sb–C(31)	97.80(5)	C(43)–C(44)–C(45)	120.4(2)
C(11)–Sb–C(41)	95.35(5)	C(44)–C(45)–C(46)	120.0(2)
C(21)–Sb–C(31)	115.24(5)	C(41)–C(46)–C(45)	119.0(2)
C(21)–Sb–C(41)	121.90(5)	C(42)–C(41)–C(46)	120.8(1)
C(31)–Sb–C(41)	118.00(6)	P–O(1)···Sb	92.96(5)
C(12)–C(11)–Sb	117.4(1)	C(1)–O(1)···Sb	126.0(1)
C(16)–C(11)–Sb	123.5(1)	S(1)–Sb···O(1)	50.83(2)
C(13)–C(12)–C(11)	120.6(2)	C(11)–Sb···O(1)	132.94(4)
C(14)–C(13)–C(12)	119.9(2)	C(21)–Sb···O(1)	68.73(4)
C(15)–C(14)–C(13)	120.0(2)	C(31)–Sb···O(1)	128.93(4)
C(14)–C(15)–C(16)	120.7(2)	C(41)–Sb···O(1)	60.71(4)

The structures were solved using direct methods and refined by least-squares calculation in anisotropic approximation for non-hydrogen atoms. Hydrogen atoms were added at ideal positions and refined using a riding model. Data collection and editing, as well as refinement of unit cell parameters, was performed with the SMART and SAINT-plus program packages [9]. Structure solution and refinement were performed with the SHELXTL/PC program packages [10]. Selected bond lengths and angles are listed in Tables 2 and 3. Complete crystallographic details are included in the Supporting Information.

3. Results and discussion

3.1. Heteronuclear (^{13}C, ^{31}P) CP/MAS NMR data

Experimental ^{13}C CP/MAS NMR spectra of polycrystalline *O*,*O*′-dialkyldithiophosphate tetraphenylantimony(V) complexes are presented in Fig. 1. There are two expected groups of ^{13}C resonance lines from (i) alkyl substituents at the oxygen atoms of Dtph ligands and (ii) =C= and =CH– groups of four aromatic C_6H_5-rings in

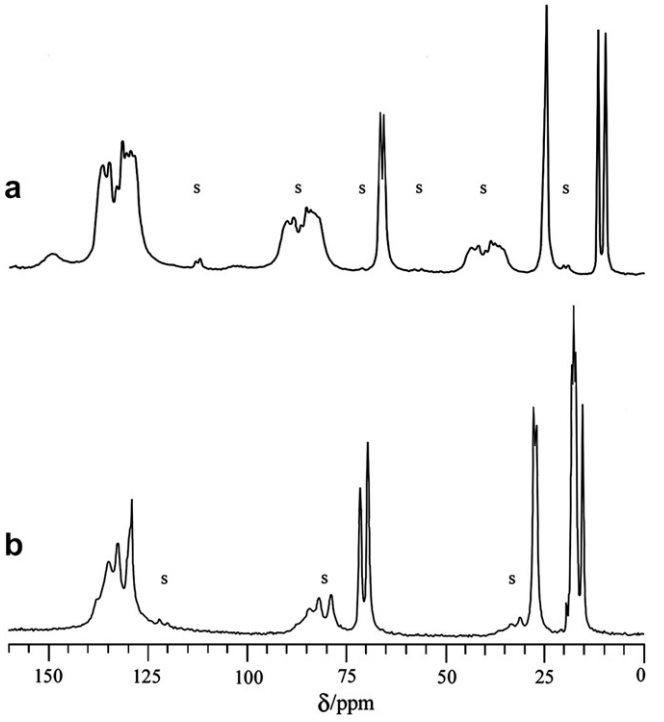

Fig. 1. 90.52 MHz ^{13}C CP/MAS NMR spectra of polycrystalline *O*,*O*′-dipropyldithiophosphate- (a) and *O*,*O*′-di-*iso*-butyldithiophosphate- (b) tetraphenylantimony(V) complexes. The MAS frequencies were 4.2 in (a) and 4.5 kHz in (b). The number of transients was 7500 and 3600 in (a) and (b), respectively. (The sidebands are denoted by 's'.)

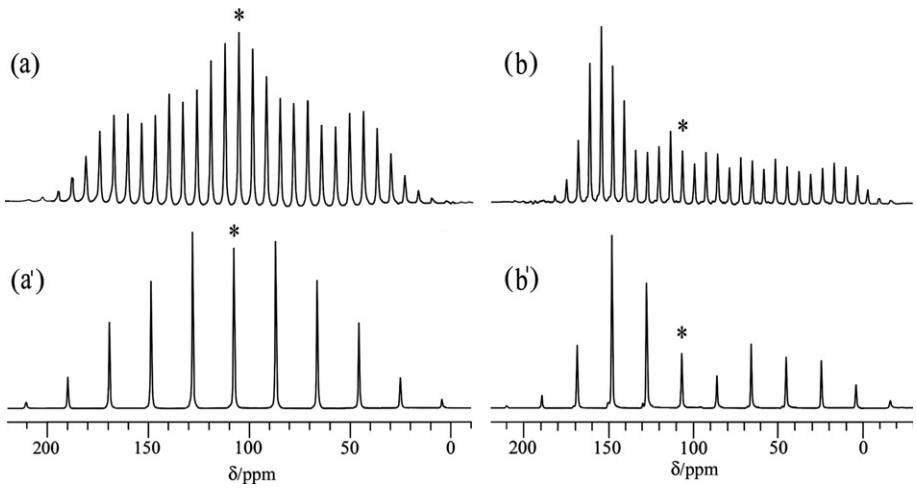

Fig. 2. 145.73 MHz ^{31}P CP/MAS NMR spectra of polycrystalline *O,O′*-dialkyldithiophosphate tetraphenylantimony(V) complexes: [$Sb(C_6H_5)_4${$S_2P(OC_3H_7)_2$}] (a) and (a′); [$Sb(C_6H_5)_4${$S_2P(O$-*i*-$C_4H_9)_2$}] (b) and (b′). (The central bands are denoted by asterisks.) The MAS frequencies were 1.0 and 3.0 kHz in (a), (b) and (a′), (b′), respectively. The number of transients was 380 in (a), 128 in (a′), 1680 in (b) and 2000 in (b′).

the discussed spectra of both complexes **1** and **2**. Pairs of highly shielded ^{13}C resonance lines, which appear between 9.5 and 67 ppm (compound **1**) and 17.5 and 73 ppm (**2**), are assigned to –OCH_2–, –CH_2–, –CH═ and –CH_3 groups in Dtph ligands. They have almost equal integral intensities that suggests a structural inequivalence in the neighbouring chains of alkyl substituents at the oxygen atoms. In contrast, aromatic C_6H_5– rings have poorly shielded ^{13}C sites with chemical shift values laying within the ranges of 128.6–149.4 and 129.7–138.4 ppm for compounds **1** and **2**, respectively. (The most deshielded resonance line at ~150 ppm assigned to the carbon atom directly bound to the antimony atom in **1** is not observed in **2** because of a severe line broadening.) This assignment is in accord with previously reported ^{13}C chemical shifts for carbon sites in phenyl groups of polycrystalline heteroleptic *N,N*-dialkyldithocarbamate tetraphenylantimony(V) complexes [3,4].

Fig. 2 displays ^{31}P CP/MAS NMR spectra of both polycrystalline compounds **1** (Figs. 2a and 2a′) and **2** (Figs. 2b and 2b′) obtained at two different spinning frequencies (1 and 3 kHz). Isotropic chemical shifts for phosphorus sites in these compounds can be read from the positions of the centrebands (marked by asterisks in Fig. 2), which are flanked by the spinning sidebands. In each ^{31}P MAS NMR spectrum, only one centreband resonance line was observed that suggests unique structural positions of the phosphorus atoms in each of the two *O,O′*-dialkyldithiophosphate tetraphenylantimony(V) complexes. A comparative analysis of isotropic ^{31}P chemical shift values for the above heteroleptic antimony(V) complexes and the initial potassium dialkyldithiophosphates (see Table 4) reveals more shielded phosphorus sites (smaller values in the deshielding δ-scale) in the former case. This result corresponds to our previous ^{31}P NMR studies performed for *O,O′*-dialkyldithiophosphate complexes of various bivalent transition metals [11–20]. Therefore, the formation of covalent bonds of dithiophosphate groups with the antimony atom is the origin of the observed additional shielding.

Table 4
^{31}P[a] NMR chemical shift tensor parameters for *O,O′*-dialkyldithiophosphate tetraphenylantimony(V) complexes

Compound	^{31}P		
	δ_{iso} (ppm)	δ_{aniso} (ppm)[b]	η[b]
(**1**) [$Sb(C_6H_5)_4${$S_2P(OC_3H_7)_2$}]	107.6	−84.1 ± 0.4	0.98 ± 0.01
(**2**) [$Sb(C_6H_5)_4${$S_2P(O$-*i*-$C_4H_9)_2$}]	106.8	−117.0 ± 0.7	0.12 ± 0.03
(**1a**) K{$S_2P(OC_3H_7)_2$} [18]	114.7	−106 ± 3	0.1 ± 0.1
	114.5 (1:1)	−109 ± 4	0.23 ± 0.14
(**2a**) K{$S_2P(O$-*i*-$C_4H_9)_2$} [18]	110.9	−123.0 ± 2.0	0.0 ± 0.1

[a] Relative to 85.5% H_3PO_4, deshielding scale.
[b] $\delta_{aniso} = \delta_{zz} - \delta_{iso}$; $\eta = (\delta_{yy} - \delta_{xx})/(\delta_{zz} - \delta_{iso})$.

In spite of the close ^{31}P isotropic chemical shift values (see Table 4), compounds **1** and **2** have remarkably different shapes of the spinning sideband patterns in their ^{31}P CP/MAS NMR spectra (Fig. 2) that points out at large differences in ^{31}P chemical shift anisotropies (**CSA**) of phosphorus sites in these molecular systems. These kinds of MAS ^{31}P NMR spectral pattern reflect, undoubtedly, either mainly rhombic or almost axially symmetric characters of the ^{31}P chemical shift tensor (**CST**) of phosphorus sites in the cases **1** and **2**, respectively. Moreover, our previous ^{31}P MAS NMR studies of *O,O′*-dialkyldithiophosphate zinc(II) [11,12,18], nickel(II) [16,18], cadmium(II) [13–15,20] and lead(II) [17,19] complexes allowed us to conclude with confidence, that principally different coordination modes of Dtph groups in the complexes **1** and **2** are in the basis of these differences in ^{31}P CSTs.

To confirm the validity of this conclusion based on ^{31}P CP/MAS NMR data, the molecular structures of the

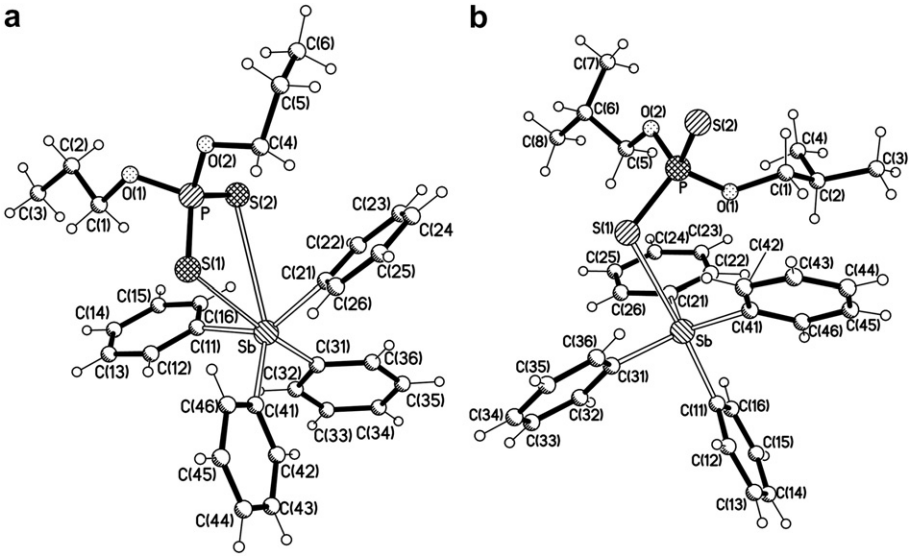

Fig. 3. Molecular structures of complexes **1**, $[Sb(C_6H_5)_4\{S_2P(OC_3H_7)_2\}]$ (a) and **2**, $[Sb(C_6H_5)_4\{S_2P(O\text{-}i\text{-}C_4H_9)_2\}]$ (b).

complexes **1** and **2** were resolved by the direct method, the single-crystal X-ray diffraction data analysis.

3.2. Structural description of $[Sb(C_6H_5)_4\{S_2P(OC_3H_7)_2\}]$ (1) and $[Sb(C_6H_5)_4\{S_2P(O\text{-}i\text{-}C_4H_9)_2\}]$ (2)

The molecular structures resolved for the heteroleptic tetraphenylantimony(V) complexes **1**, $[Sb(C_6H_5)_4\{S_2P(OC_3H_7)_2\}]$ and **2**, $[Sb(C_6H_5)_4\{S_2P(O\text{-}i\text{-}C_4H_9)_2\}]$ are shown in Fig. 3; selected bond lengths and angles are given in Tables 2 and 3. There are four and two discrete structurally equivalent molecules in the unit cells of complexes **1** and **2**, respectively. In each discussed compound, the central antimony atom links four phenyl planar rings and one *O*,*O*′-dialkyldithiophosphate ligand. Nevertheless, different types of geometry have been established for the aforementioned molecules. The distorted octahedral chromophore $[SbC_4S_2]$ and the trigonal bipyramidal one $[SbC_4S]$ were discovered in the molecular structures **1** and **2**, respectively. These unexpected structural distinctions between chemically related compounds are defined by the principally different coordination modes of *O*,*O*′-dipropyldithiophosphate and *O*,*O*′-di-*iso*-butyldithiophosphate ligands in their molecular structures (i.e., a bidentate chelating and an unidentate coordination, respectively).

Let us examine the molecular structures of compounds **1** and **2** in detail. There are four planar phenyl rings and *S*-unidentately coordinated *O*,*O*′-di-*iso*-butyldithiophosphate ligand in the inner coordination sphere of complex **2** (Fig. 3b). These exhibit a distorted trigonal bipyramidal neighbouring environment of the antimony atom (with the coordination number equal to 5). Three phenyl rings forming the short chemical bonds Sb–C(21, 31, 41) (2.104–2.115 Å, see Table 2) are in the equatorial plane of the discussed trigonal bipyramid, while the fourth, less strongly bound, phenyl ring: Sb–C(11) 2.147 Å and the Dtph group: Sb–S(1) 2.9092 Å define two axial positions. In the antimony distorted trigonal bipyramidal polyhedron, the central atom is 0.2706 Å shifted out of the mean $[S_3]$ plane towards the axial carbon atom C(11). The C(11)–Sb–S(1) angle is equal to 176.23° that is close to the corresponding value in the ideal trigonal bipyramid (TBP) −180°. However, the observed deviation of this angle from 180° indicates some contribution of a tetragonal pyramid (TP) to the geometry of the antimony coordination polyhedron $[SbC_4S]$. To characterise the geometry of discussed coordination polyhedron quantitatively, the τ-descriptor was used in our analysis. This τ-descriptor has been suggested by Addison et al. [21] as a convenient parameter and defined using the following equation $\tau = (\alpha - \beta)/60$ (in our case, α and β are the two largest L–Sb–L angles, $\alpha > \beta$). In an ideal TP (C_{4v}), $\tau = 0$ since $\alpha = \beta$. In a regular TBP (C_{3v}), the axial L–Sb–L angle (α) is equal to 180°, while the equatorial angle (β) is 120° giving rise to $\tau = 1$. A polyhedron manifold with contributions from 100% TBP to 100% TP corresponds to τ values falling within the range 1–0. In molecule **2**, the two largest L–Sb–L angles: C(11)–Sb–S(1) and C(21)–Sb–C(41) are equal to 176.23° and 121.90°, respectively (see Table 3). Therefore, $\tau = 0.9055$, which point to 90.55% and 9.45% contributions of TBP and TP, respectively, to a geometry of the antimony coordination polyhedron.

In complex **1**, whose structure is shown in Fig. 3a, the central antimony atom is bound with four carbon atoms of phenyl groups and with both sulphur atoms of the Dtph group, defining the six-fold coordination and exhibiting a distorted octahedral molecular structure. Hence, in contrary to complex **2**, *O*,*O*′-dipropyldithiophosphate ligand displays a bidentate coordination mode in the molecular structure of **1**. The central metal atom links three phenyl groups by short chemical bonds Sb–C(11, 21, 41) (2.123–2.128 Å, see Table 3) and by one, weakly bound, sulphur

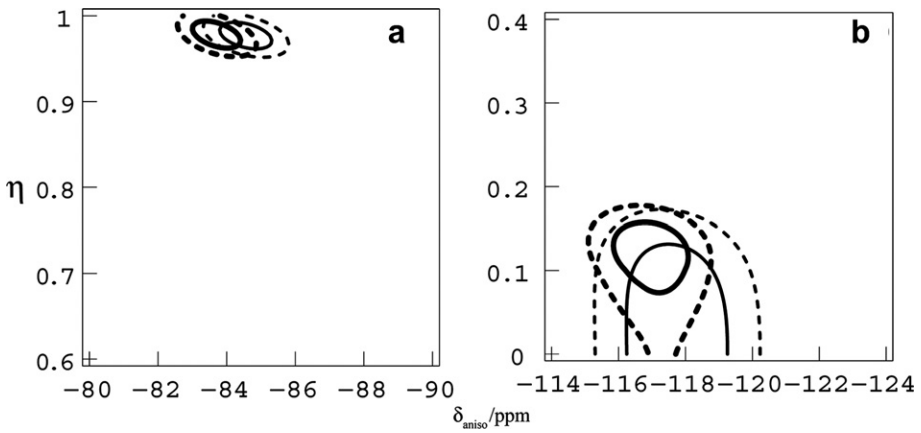

Fig. 4. χ^2 statistics as a function of the ^{31}P CSA parameters δ_{aniso} and η. Graphs for $[Sb(C_6H_5)_4\{S_2P(OC_3H_7)_2\}]$ (a) and $[Sb(C_6H_5)_4\{S_2P(O\text{-}i\text{-}C_4H_9)_2\}]$ (b) are presented. The 68.3% joint confidence limit (solid) and 95.4% joint confidence limit (dashed) for the two CSA parameters are shown. In each case (a) and (b) simulations were performed for one P-site but at two different spinning frequencies: 2 kHz (thick lines) and 3 kHz (thin lines).

atom Sb–S(2) 3.5571 Å in the equatorial plane of the distorted octahedron. The fourth, less strongly bound, phenyl ring: Sb–C(31) 2.149 Å and the other sulphur atom: Sb–S(1) 3.0060 Å are in the axial positions. The axial S(1) and C(31) atoms have an S–Sb–C angle 172.27° that is noticeably deviated from the ideal value of 180°.

The bidentate coordination mode of the *O*,*O*′-dipropyldithiophosphate ligand leads to formation of a four-membered chelate ring [SbS_2P]. This ring is characterised by an almost planar geometry that is supported by values of P–S–S–Sb and S–Sb–P–S torsion angles (178.2° and 178.3°, respectively). The dithiophosphate group is essentially anisobidentate: one of the sulphur atoms forms a rather strong chemical bond – S(1)–Sb 3.0060 Å, while the other one is weakly bound to the central Sb atom – S(2)–Sb 3.5571 Å.

Hence, the principally different coordination modes of *O*,*O*′-dipropyl- and *O*,*O*′-di-*iso*-butyldithiophosphate ligands to the central antimony atom (i.e., a bidentate chelating and an unidentately coordinated, respectively) are in the basis of all main structural distinctions between these chemically related compounds **1** and **2**.

3.3. Correlations between ^{31}P chemical shift anisotropy and S–P–S angle

Previously, we reported on crystalline dialkyldithiophosphate nickel(II), zinc(II), cadmium(II) and lead(II) complexes of mononuclear, binuclear and polynuclear molecular structures [11–20]. Dtph groups in these compounds have either terminal chelating or/and bidentate bridging or/and combined (tridentate bridging) structural functions. Using X-ray diffraction, ^{31}P NMR data and ab initio quantum mechanical calculations on the above systems, we have found empirical correlations between the S–P–S angle and the principal components of the ^{31}P chemical shift tensor (CST): for large S–P–S angles (characteristic for bridging Dtph ligands) the tensor is prolate (δ_{22} is close to δ_{11}, $\delta_{aniso} < 0$),[1] while for small S–P–S angles (specific for terminal chelating Dtph ligands) the ^{31}P CST is oblate (δ_{22} is close to δ_{33}, $\delta_{aniso} > 0$) [18,19].

However, newly prepared here heteroleptic antimony(V) complex **2** comprises another type of binding, i.e. an unidentate coordination of the *O*,*O*′-di-*iso*-butyldithiophosphate ligand to the central atom. This type of binding is characterised by a large S–P–S angle, which is close to 120° as in ionic Dtph compounds with an essential contribution of the double bond character in one of the two P–S bonds.

To characterise quantitatively phosphorus sites in both the bidentate chelating and the unidentately coordinated Dtph ligands of the heteroleptic tetraphenylantimony(V) complexes **1** and **2**, both ^{31}P isotropic chemical shifts, δ_{iso}, and the ^{31}P chemical shift anisotropy (CSA) parameters were implemented. To evaluate ^{31}P CSAs, relative intensities of sidebands in spinning sideband manifolds (see Fig. 2) were incorporated in the Mathematica program developed by Levitt and co-workers [8]. This program calculates χ^2-statistics as a function of the two ^{31}P CSA parameters: the chemical shift anisotropy, specified as $\delta_{aniso} = \delta_{zz} - \delta_{iso}$, and the asymmetry parameter of the chemical shift tensor, $\eta = (\delta_{yy} - \delta_{xx})/(\delta_{zz} - \delta_{iso})$. The global minimum of this statistics, χ^2_{min}, gives values for the two CSA parameters, δ_{aniso} and η, while the joint confidence limit is the measure of errors for these parameters [8]. Fig. 4 shows joint confidence limits for δ_{aniso} and η, while ^{31}P CSA data given in Table 4 correspond to the minima on χ^2-plots [8]. (It is necessary to note that the zero asymmetry parameter, $\eta = 0$, corresponds to an axially symmetric CST, while an increase of the η-value from 0 to 1 reflects a rise in the rhombicity of the CST.) In spite of close ^{31}P isotropic chemical shifts, δ_{iso}, for P-sites in Dtph ligands of complexes **1** and **2**, two ^{31}P CSTs are

[1] Defined as $\delta_{11} > \delta_{22} > \delta_{33}$; $\delta_{aniso} = \delta_{zz} - \delta_{iso}$; $\eta = (\delta_{yy} - \delta_{xx})/(\delta_{zz} - \delta_{iso})$; $|\delta_{zz} - \delta_{iso}| > |\delta_{xx} - \delta_{iso}| > |\delta_{yy} - \delta_{iso}|$, i.e., $\delta_{yy} = \delta_{22}$, $\delta_{zz} = \delta_{11}$ or δ_{33}, and $\delta_{xx} = \delta_{33}$ or δ_{11}.

remarkably different (see Fig. 4 and Table 4). As expected from the general shapes of the spinning sideband patterns in ^{31}P CP/MAS NMR spectra of **1** and **2**, one of ^{31}P CST (for **1**) displays a profoundly rhombic character: $\eta = 0.98$ and $\delta_{aniso} = -84.1$ ppm, while the other one (for **2**) is an almost axially symmetric prolate tensor: $\eta = 0.12$ and $\delta_{aniso} = -117.0$ ppm (see also Fig. 4 and Table 4). Furthermore, previously, we have reported on the sign correlation of δ_{aniso} with the S–P–S angle values [18]. Moreover, in a range of negative δ_{aniso} values, it was shown that the higher $|\delta_{aniso}|$ values correspond to the larger S–P–S angles. In our cases **1** and **2**, $|\delta_{aniso}| = 84.1$ ppm correlates with the smaller S–P–S angle 116.39° (for **1**) and $|\delta_{aniso}| = 117.0$ ppm corresponds to the larger S–P–S angle 117.62° (for **2**), that is in a good agreement with our previous ^{31}P MAS NMR studies [11–20].

4. Conclusions

Crystalline heteroleptic *O*,*O*′-dipropyl- (**1**) and *O*,*O*′-di-*iso*-butyldithiophosphate (**2**) tetraphenylantimony(V) complexes were studied by means of heteronuclear ^{13}C, ^{31}P CP/MAS NMR spectroscopy and single-crystal X-ray diffraction. Discrete molecules of prepared complexes **1** and **2** are characterised by a distorted octahedral and a trigonal bipyramidal geometries, respectively. These unexpected structural differences between similar compounds are governed by different coordination modes of *O*,*O*′-dipropyl- and *O*,*O*′-di-*iso*-butyldithiophosphate ligands to antimony atoms in the molecular structures of **1** and **2** (i.e. *S*,*S*′-bidentate chelating and *S*-unidentately coordinated, respectively). The ^{31}P chemical shift anisotropy parameters, δ_{aniso} and η, are remarkably different for phosphorus sites in these two species of Dtph ligands. The ^{31}P CST is mainly rhombic ($\eta = 0.98$) in **1**, while it is almost axially symmetric prolate tensor in **2** ($\eta = 0.12$). The ^{31}P CST data correlate with differences in S–P–S bond angles in these molecular systems: 116.39° and 117.62° in **1** and **2**, respectively, in accord with previously reported ab initio quantum mechanical calculations for a model $[(CH_3O)_2PS_2]^-$ molecular fragment [18].

Acknowledgments

This work has been financially supported by Agricola Research Centre at Luleå University of Technology and granted by the Russian Foundation of Fundamental Research and the Far East Division of the Russian Academy of Sciences (project No. 06-0396009). We are grateful to 'CHEMINOVA AGRO A/S' for dithiophosphate chemicals, which were kindly supplied for this study. The CMX-360 spectrometer was purchased with a grant from the Swedish Council for Planning and Coordination of Research (FRN). We thank the foundation to the memory of J.C. and Seth M. Kempe for a grant from which a part of the NMR equipment has been purchased.

Appendix A. Supplementary material

CCDC 607257 and 607258 contain the supplementary crystallographic data (excluding structure factors) for this paper. These data can be obtained free of charge via http://www.ccdc.cam.ac.uk/conts/retrieving.html, or from the Cambridge Crystallographic Data Centre, 12 Union Road, Cambridge CB2 1EZ, UK; fax: (+44) 1223-336-033; or e-mail: deposit@ccdc.cam.ac.uk. Supplementary data associated with this article can be found, in the online version, at doi:10.1016/j.ica.2007.02.044.

References

[1] N.S. Zefirov (Ed.), Khimicheskaya entsiklopediya (Chemical Encyclopedia), vol. 4, Bol'shaya Russ. Entsiklopediya, Moscow, 1995, p. 447.
[2] V.V. Sharutin, O.K. Sharutina, T.P. Platonova, A.P. Pakusina, A.V. Gerasimenko, E.A. Gerasimenko, B.V. Bukvetsky, D.Ju. Popov, Russ. J. Coord. Chem. (Engl. Transl.) 29 (2003) 13.
[3] A.V. Ivanov, A.P. Pakusina, M.A. Ivanov, V.V. Sharutin, A.V. Gerasimenko, O.N. Antzutkin, G. Gröbner, W. Forsling, Dokl. Phys. Chem. (Proc. Russ. Acad. Sci.) (Engl. Transl.) 401 (2005) 44.
[4] V.V. Sharutin, M.A. Ivanov, A.V. Gerasimenko, A.V. Ivanov, A.P. Pakusina, O.N. Antzutkin, W. Forsling, G. Gröbner, Russ. J. Coord. Chem. (Engl. Transl.) 32 (2006) 387.
[5] A. Pines, M.G. Gibby, J.S. Waugh, J. Chem. Phys. 56 (1972) 1776.
[6] W.L. Earl, D.L. VanderHart, J. Magn. Reson. 48 (1982) 35.
[7] K. Karaghiosoff, in: D.M. Grant, R.K. Harris (Eds.), Encyclopedia of Nuclear Magnetic Resonance, vol. 6, Wiley, New York, 1996, p. 3612.
[8] O.N. Antzutkin, Y.K. Lee, M.H. Levitt, J. Magn. Reson 135 (1998) 144.
[9] Bruker, SMART and SAINT-Plus, Versions 5.0. Data Collection and Processing Software for the SMART System, Bruker AXS Inc., Madison, Wisconsin, USA, 1998.
[10] Bruker, SHELXTL/PC, Versions 5.10, An Integrated System for Solving, Refining and Displaying Crystal Structures From Diffraction Data, Bruker AXS Inc., Madison, Wisconsin, USA, 1998.
[11] A.V. Ivanov, W. Forsling, M. Kritikos, Antzutkin, A.-C. Larsson, F.A. Zhukov, Z.F. Jusupov, Dokl. Chem. (Proc. Russ. Acad. Sci.) (Engl. Transl.) 375 (2000) 236.
[12] A.V. Ivanov, O.N. Antzutkin, A.-C. Larsson, M. Kritikos, W. Forsling, Inorg. Chim. Acta 315 (2001) 26.
[13] A.V. Ivanov, O.N. Antzutkin, W. Forsling, D. Boström, Y.-G. Yin, N.A. Rodionova, Dokl. Phys. Chem. (Proc. Russ. Acad. Sci.) (Engl. Transl.) 387 (2002) 299.
[14] Y.-G. Yin, W. Forsling, D. Boström, O.N. Antzutkin, M. Lindberg, A.V. Ivanov, Chin. J. Chem. 21 (2003) 291.
[15] A.V. Ivanov, O.N. Antzutkin, W. Forsling, N.A. Rodionova, Russ. J. Coord. Chem. (Engl. Transl.) 29 (2003) 301.
[16] A.V. Ivanov, A.-C. Larsson, N.A. Rodionova, A.V. Gerasimenko, O.N. Antzutkin, W. Forsling, Russ. J. Inorg. Chem. (Engl. Transl.) 49 (2004) 373.
[17] A.-C. Larsson, A.V. Ivanov, O.N. Antzutkin, A.V. Gerasimenko, W. Forsling, Inorg. Chim. Acta 357 (2004) 2510.
[18] A.-C. Larsson, A.V. Ivanov, W. Forsling, O.N. Antzutkin, A.E. Abraham, A.C. de Dios, J. Am. Chem. Soc. 127 (2005) 2218.
[19] A.-C. Larsson, A.V. Ivanov, K.J. Pike, W. Forsling, O.N. Antzutkin, J. Magn. Reson. 177 (2005) 56.
[20] A.V. Ivanov, A.V. Gerasimenko, O.N. Antzutkin, W. Forsling, Inorg. Chim. Acta 358 (2005) 2585.
[21] A.W. Addison, T.N. Rao, J. Reedijk, J. van Rijn, G.C. Verschoor, J. Chem. Soc., Dalton Trans. 7 (1984) 1349.